Open access • Journal Article • DOI:10.1007/S10653-014-9667-7

Comparison of physical and chemical properties of ambient aerosols during the 2009 haze and non-haze periods in Southeast Asia — Source link

Jingsha Xu, Xuhong Tai, Raghu Betha, Jun He ...+1 more authors

Institutions: The University of Nottingham Ningbo China, National University of Singapore

Published on: 01 Oct 2015 - Environmental Geochemistry and Health (Springer Netherlands)

Topics: Haze and HYSPLIT

Comparison of physical and chemical properties of ambient aerosols during the 2009 haze and non-haze periods in Southeast Asia

Jingsha Xu[1, 2], Xuhong Tai[3], Raghu Betha[3], Jun He [2*], Rajasekhar Balasubramanian[3§]

[1] International Doctoral Innovation Centre, The University of Nottingham Ningbo China, Ningbo 315100, China

[2] Department of Chemical and Environmental Engineering, The University of Nottingham Ningbo China, Ningbo 315100, China

[3] Department of Civil and Environmental Engineering, National University of Singapore, Singapore

Correspondence to:

*Dr Jun He at: jun.he@nottingham.edu.cn or

[§]Dr Rajasekhar Balasubramanian at: ceerbala@nus.edu.sg

Abstract

Recurrent smoke haze episodes that occur in Southeast Asia (SEA) are of much concern because of their environmental and health impacts. These haze episodes are mainly caused by uncontrolled biomass and peat burning in Indonesia. Airborne particulate matter (PM) samples were collected in the Southwest (SW) coast of Singapore from 16 August to 9 November in 2009 to assess the impact of smoke haze episodes on the air quality due to the long-range transport of biomass and peat burning emissions., The physical and chemical characteristics of PM were investigated during pre-haze, smoke-haze, and post-haze periods. Days with $PM_{2.5}$ mass concentrations of ≥ 35 μg m^{-3} were considered as smoke-haze events. Using this criterion, out of the total 82 sampling days, 9 smoke-haze events were identified. The origin of air masses during smoke haze episodes was studied on the basis of HYPSLIT backward air trajectory analysis for 4 days. In terms of the physical properties of PM, higher particle surface area concentrations (PSAC) and particle gravimetric mass concentrations (PGMC) were observed during the smoke-haze period, but there was no consistent pattern for particle number concentrations (PNC) during the haze period as compared to the non-haze period except that there was a significant increase at about 08:00, which could be attributed to the entrainment of PM from aloft after the break-down of the nocturnal inversion layer. As for the chemical characteristics of PM, among the six key inorganic water-soluble ions (Cl^-, NO_3^-, nss-SO_4^{2-}, Na^+, NH_4^+, and nss-K^+) measured in this study, NO_3^-, nss-SO_4^{2-}, and NH_4^+ showed a significant increase in their concentrations during the smoke-haze period together with nss-K^+. These observations suggest that the increased atmospheric loading of PM with higher surface area and increased concentrations of optically active secondary inorganic aerosols $(NH_4)_2SO_4$ or NH_4HSO_4 and NH_4NO_3) resulted in the atmospheric visibility reduction in SEA due to the advection of biomass and peat burning emissions.

Keywords: Haze aerosol · Biomass burning · Physical properties · Inorganic ions.

Introduction

Atmospheric haze (reduced visibility), caused by increased loading of aerosols, has a strong impact on the radiative balance of the Earth by direct reflection and absorption of incoming solar radiation or by indirect reflection due to cloud formation (IPCC 2007; Jacobson 2004; Pandis and Seinfeld 1998). It is known that the haze phenomenon is caused by either natural sources such as volcanic eruptions and naturally ignited fires, or anthropogenic sources such as fossil fuel related combustion, uncontrolled biomass burning, biofuel burning, land use changes for agriculture or developments, or a combination of both (He et al. 2010; Jacobson 2004). The chemical composition of haze aerosols depends largely on the fuel type, combustion phase (flaming vs. smoldering), duration and intensity of combustion, and prevailing meteorological conditions (Reid et al. 2005). Generally, haze aerosols contain both primary particulates emitted directly into the atmosphere and secondary particulates formed from gaseous precursors emitted, the relative proportion of which would change over time and distance. Although the general residence time of ambient fine aerosols is usually > 5 days, at about 1 to 2 weeks with age, it is still much shorter than that of greenhouse gases. Nevertheless, the average transport distance over which aerosols are transported is estimated to be ≥ 1000 km, leading to potentially large regions that can be affected by the influence of haze when there is extensive biomass burning over a wide area (Brook et al. 2007).

Smoke haze episodes occur in Southeast Asia (SEA) annually due to recurrent slash and burn agricultural activities, but with different intensities and impacts from year to year depending on weather conditions. As SEA's air quality is influenced by local particle emissions heavily, the SEA haze becomes a complex regional air pollution problem, due to the intermixing of haze particles with fossil fuel-derived particles, with the following impacts. The physical, chemical and optical properties of the SEA haze can affect the ecosystems, human health, climate change and water budget in the affected regions (Ramanathan et al. 2005; Sundarambal et al. 2010). The reduction of atmospheric visibility can vary from 20% to 90% depending on the intensity of haze episodes and the characteristics of aerosols contained in them (Wang 2002). Severe smoke-haze episodes can also indirectly affect the efficiency of vegetative photosynthesis. When water insoluble aerosols deposited on leaves are not washed off by precipitation, they could lead to a reduction of as much as 35%

photosynthesis with lower crop yields, lesser CO_2 removal and eventual increase in greenhouse effects (Bergin et al. 2001; Tang 1996). In terms of regional climate change, with the high emission of light absorbing aerosol particulates into the atmosphere, greenhouse effects are expected to increase due to the concurrent increase of greenhouse gases emitted, even when the aerosol's short-term cooling effects are considered in the radiative budget (Jacobson 2004). The massive concurrent emissions of CO_2 from biomass burning together with aerosols have been linked to the prolonged duration of the regional La Nina effects (unusually cold and wet weather conditions in SEA) (Van der Werf 2008). The increased smoke particle concentration associated with smoke-haze episodes could also affect cloud cover and the cloud chemistry (Geresdi et al. 2006; Reid et al. 2005). Strong associations between increased aerosol concentrations and health effects have been observed during the regional smoke-haze episodes over the years. On average, a nearly six fold increase in emergency visits for acute asthma exacerbation were observed for every 20 $\mu g\ m^{-3}$ increase of the total suspended particles (TSP) from 78 $\mu g\ m^{-3}$ (Chew et al. 1999).

Dry weather conditions in SEA over the months of June to October 2009, exacerbated by the El Niño Southern Oscillation (ENSO), increased the likelihood of massive uncontrolled burning due to prolonged droughts (Gnanaseelan and Vaid 2010; Aiken 2004). The sampling site was influenced by the southwest (SW) winds from August to October. In view of a range of environmental and health impacts associated with smoke-haze periods, it is important to characterize the physical and chemical properties of haze and non-haze aerosols in SEA so that appropriate environmental policies and practical mitigation strategies can be developed to protect sensitive ecosystems and human health. Therefore, a field sampling campaign was conducted in the Southwest (SW) coast of Singapore from 16 August to 9 November in 2009. This study aimed at investigating both physical and chemical properties of haze aerosols in relation to those of background aerosols. In addition, backward trajectory analysis was carried out to assess the influence of air masses of different origins on the aerosol physical and chemical properties as well.

Methods

Sample Collection

Particulate sampling was carried out from 16 August 2009 to 9 November 2009, beginning at 09:00 (UTC+8 hrs) till the following day. The sampling site (1° 18' N, 103° 46' E) is located at an altitude of 67 m above sea level at the roof of block E2 in the National University of Singapore (NUS). Singapore (1° 18' N, 103° 50' E) is situated at the tip of Peninsula Malaysia and within the regional influences of SEA smoke-haze with a total area of 693 km^2. The sampling site is considered to be an urban background location where the local air quality is influenced largely by vehicular traffic on the major expressway (Ayer Rajah Expressway) and industrial emissions from petroleum, petrochemical, and specialty chemical industries located on Jurong Island, 5 to 10 km on the southwest of this site. The sampling site is also influenced by the long-range transport of smoke-haze impacted air masses from Sumatra, Indonesia (Balasubramanian et al. 2003; Balasubramanian et al. 1999).

$PM_{2.5}$ were collected by 2 Mini-Vol Portable Samplers (MPSs) (AirMetrics, US) running in parallel with Teflon membrane filters at the flow rate of 6 $Lmin^{-1}$ for 24-hrs. The filter sample collection was performed periodically in every 1-in-6 days with additional sample collections performed when smoke-haze episodes were observed. Before and after the sampling, all the filters were equilibrated under the conditions with 22 ± 1°C with controlled relative humidity (RH) of 35% for 24 hours right before they were weighed with a MC5 microbalance (Sartorius AG) accurate to 1μg. Meanwhile, subsets of both filters were stored and analyzed as laboratory blanks.

Physical Measurements of Atmospheric Aerosols

The particle number concentration and size distribution were measured by a real-time Fast Mobility Particle Sizer (FMPS, TSI-3091d, TSI.) with a mobility diameter range of 5.6 to 560 nm, which is able to scan the number concentration of a poly-disperse, heterogeneous aerosol particle system for the nuclei and accumulation (sub-micron) mode based upon electrical-based measurements for particle counting. Data were recorded every second throughout the sampling period. TSI Dust Track™ II Aerosol Monitor was utilized to measure the real-time mass concentration of $PM_{2.5}$ atmospheric particles by photometric measurements based on the Mie scattering theory. The Dust Track device was calibrated with reference to the gravimetric data

obtained from the MPS operated in parallel for a duration of 30-days using Teflon membrane filters. Twice daily auto zero checks were performed with filtered atmospheric air to reduce background noise influences. The Dust Track device was operated at a flow rate of 3.0 L min^{-1}, and the recorded data were analyzed at 5-min averages. The accuracy of the Dust Track measurements was improved by eliminating positive artefacts of photometric measurements due to water vapor (Jakubczyk et al. 2005; Ter-Avetisyan et al. 2003). With a reasonable correlation of 0.446 and R^2 of 0.82, the collected data from the Dust Track device was classified and analyzed for both smoke-haze and non-haze periods.

Chemical Analysis of Atmospheric Aerosols

Three-quarters of the Telfon filter was extracted by ultra-sonication (Elmasonic, S 60H) with 12 ml of ultra-pure deionized water and the extract was filtered through Target® 30 mm syringe filters with 0.45 µm Teflon membrane.. After this step, the extracts were processed for the Ion Chromatography(IC) analysis. All filter samples extracted and the ones remaining after chemical analysis were stored in individual vials at 4°C for future analysis. In this study, six inorganic ions from the aerosol extracts: Cl^-, NO_3^-, SO_4^{2-}, Na^+, NH_4^+ and K^+ were quantified by the Ion Chromatography (Dionex ICS-2000) and the detection is based on the concept of conductivity detection of either anions or cations by suppression, separated over individual retention times.

Air Mass Backward Trajectory Analysis

The latest, updated Hybrid Single-Particle Lagrangian Integrated Trajectory (HYSPLIT) model (Version 4.9) (Draxler 2013; Rolph 2013), developed by the National Oceanic and Atmospheric Administration (NOAA), was used to compute backward trajectories for air samples collected in this study. Meteorological data were obtained from National Centers for Environmental Prediction (NCEP) Global Data Assimilation System (GDAS, global, 2006-present). Kinematic 3D trajectories were used as they are reported to provide an accurate description of the history of air masses in comparison with all of the other approaches (isentropic, isobaric) (Stohl 1998; Stohl and Seibert 1998). Backward air trajectories, beginning at 09:00, were generated at every 6-hrs intervals during each sampling event for 96 h back in time with 500 m-agl ending level. This atmospheric level is very frequently used (Erel et al.

2007; Lee et al. 2006) and ensures that the trajectory starts in the atmospheric boundary layer (ABL) (Dvorska et al. 2009). In addition, cluster analysis was conducted by using HYSPLIT model (version 4.9) as well to classify the trajectory groups of similar length and curvature for monsoon and pre-monsoon seasons.

Quality Control

Inconsistency in MPS measurements was verified by concurrent sampling of multiple MPSs and the comparison of the collected aerosol masses. A range of about ± 5 to 10% mass difference can be considered acceptable between MPS collections. During the entire sampling period, the filters were placed in individual polystyrene petri dishes, and handled with stainless-steel forceps, housed under an air-conditioned environment set at an average 22°C in the laboratory. After post-gravimetric analysis, filters were stored at -15°C until extraction and chemical analysis so as to prevent contamination and degradation. Quality control for the IC analysis was performed by running a series of calibration standards in step-up concentrations. An intermediate analysis of the median calibration standard was performed after analysis of every 24 samples to ensure stability and consistency of the IC accuracy. Duplicates were also performed to ensure the reproducibility of the samples of interest. Initial calibration and quality checks on FMPS were undertaken regularly. These procedures would eliminate interference from the instruments and give more reliable results.

Results and discussion

Segmentation of Clear Background Days and smoke-haze Events

From the analysis of the meteorological parameters acquired from the automated weather station deployed at the sampling site, it became clear that there was very little variation in pressure, air temperature, relative humidity and rainfall during the sampling period. These climate conditions with little variations throughout the year are quite typical in tropical countries such as Singapore (Betha et al. 2013).

Out of the 82 sampling days for the daily average Dust Track-corrected gravimetric mass concentration, 9 days were identified as hazy days when the 24-hr average $PM_{2.5}$ mass concentration was ≥ 35 μg m^{-3}. Otherwise, the remaining 73 days were considered to be clear days. This criterion was selected based on the analysis of smoke haze events reported in our previous reports (Balasubramanian et al. 2003; See

et al. 2006). The same criterion was also used for identification of smoke haze events in other countries. For example, Hu et al. (2008) reported the occurrence of smoke haze events in Atlanta, GA, caused by prescribed forest fires, when the 24-hr average $PM_{2.5}$ mass concentration exceeded the National Ambient Air Quality Standard (NAAQS) of 35 $\mu g\ m^{-3}$ (Hu et al. 2008). Smoke haze events were also identified in Malaysia using the same criterion as used in this study (Radzi bin Abas et al. 2004). Figure 1 shows the classification of smoke events in this study. A general pattern of variations in 24-hr average $PM_{2.5}$ mass concentrations observed during pre-haze, smoke-haze, and post-haze periods can be noticed. The pre-haze period lasted from 16 August 2009 to 11 September 2009 while the smoke-haze episodes occurred predominantly from mid-September to early October (12 September 2009 till 3 October 2009) followed by the post-haze period from early October to early November (4 October 2009 till 9 November 2009). In this study, pre- and post-haze periods are considered to be non-haze periods.

Air Mass Backward Trajectory Analysis

The smoke-haze air mass origins were identified based on back trajectory analysis at the elevation of 500 m-agl over 96-hrs (4-days). Representative trajectories are displayed in Figure 2 for the pre-haze, smoke-haze and post-haze periods.

As can be seen from Figure 2(a) and (d), there were only a few hotspots present over the SEA region. Aerosols during the pre-haze period at Singapore might have been influenced by those hotspots occurring in Indonesia as most air masses originated from marine sources and passed through Java Sea before arriving at Singapore. Figures 2(b) and (e), show a number of hotspots (biomass and peat-land fires) located in Sumatra and the southern part of Indonesia and a cluster of back trajectories representing the transport of biomass burning-impacted air masses over the two regions (Sumatra and southern part of Indonesia) before reaching Singapore, respectively. As can be seen from Figure 2(c), there were no visible hotspots in Sumatra or Kalimantan while Figure 2(f) shows that the air masses originated from partly terrestrial and partly oceanic sources during the post-haze period. Thus, the satellite images and the back trajectory analysis indicated that the smoke-haze episodes that occurred in Singapore from September to October 2009 were due to biomass burning in Indonesia and the subsequent long-range transport of fire emissions.

235 Comparison of Physical Properties of Aerosols between Non-haze and Haze Periods

236 Differences in the physical properties of aerosols between non-haze and haze affected
237 days were investigated by comparing the diurnal particle number concentrations
238 (PNC), particle surface area concentrations (PSAC), and particle gravimetric mass
239 concentrations (PGMC) as shown in Figure 3. Figures 3(a) and (b) show the
240 normalized concentrations of measured particle number (dN/dlogDp) and estimated
241 surface area (dS/dlogDp) concentrations during sampling days. As can be seen from
242 Figure 3(a), the average diurnal PNC was 3.31×10^5 cm^{-3} for clear days and 3.50×10^5
243 cm^{-3} for hazy days . For non-hazy days, four distinctive peaks were observed. For
244 smoke-haze days, the most significant peak was the one observed at 0800 hrs with the
245 highest PNC being $8.14\times10^5 \pm 1.29\times10^6$ cm^{-3} (mean ± SD) and also with the largest
246 standard error due to the most severe smoke-haze episode that occurred on the 27th
247 September 2009 with the maximum PNC of 3.73×10^6 cm^{-3} and with the 24-hr mean
248 of 5.37×10^5 cm^{-3}.

249 Interestingly, smoke-haze affected days had a higher PNC than that of non-hazy
250 days before 10:0.0 However, the PNC declined after 10:00 and became even lower
251 than that on non-hazy days. The decline in the PNC appears to be associated with the
252 pronounced vertical mixing of air in the presence of sunlight during day i.e. improved
253 advection and dispersion of haze particles. In addition, the removal of aerosol
254 particles by sedimentation or scavenging from the atmosphere is also possible (Reid et
255 al. 2005). For non- hazy and hazy days, the influence of local traffic and industrial
256 primary emissions is expected to be basically the same, but the significantly increased
257 atmospheric loading of pre-existing particles in smoke haze period can suppress the
258 occurrence of nucleation during the day by removing precursor gases through
259 adsorption (Betha et al. 2013). When relatively lower PNC was present during non-
260 haze period, the formation of new particles via nucleation process became favourable.
261 The competing pathways involved in the formation of new particles and the removal
262 of "aged" pre-existing particles apart from changes in atmospheric dynamics in the
263 presence of the haze layer may eventually lead to the higher number concentration of
264 particles during the daytime in the non-haze period compared to the smoke haze
265 period. We have recently reported that new particle formation (NPF) mainly occurred
266 in the afternoon (Betha et al. 2013), which may partly explain the observation of a
267 sustained high number concentration from 12:00 till 18:00 during the non-smoke

haze period in this study. A rapid increase in PNC observed from 15:00 to 16:00 with most of the particles with diameters less than 25 nm, as shown in Figure 4, supports the hypothesis about the occurrence of NPF events in the tropical atmosphere (Betha et al. 2013).

During both non-haze and haze periods, the slight general increase of PNC in the early morning hours and in the late night hours during the non-smoke haze period can be attributed to the nocturnal inversion layer that formed to decrease the mixing height, thus, increasing the ground-level PNC due to poor dispersion of ambient air. The mixing height generally increases as the day progresses with an increase in temperature. The larger fluctuations in the PNC in the early morning hours between 02:00 and 05:00 can potentially be due to changes in the strength of biomass burning emissions from the hotspots in Indonesia and/or in the long distance transboundary transport of primary aerosol particles. The distinct peak observed at 08:00 during the smoke-haze period appears to be influenced by the entrainment of haze particles from aloft (downward transport of haze particles from above the mixing height) when the nocturnal inversion layer breaks down after the sunrise (i.e. fumigation).

Figures 3(b) and (c) show distinctly higher daily mean PSAC and PGMC during the smoke-haze period. The mean PSAC measured was 4.75×10^{9} nm^2 cm^{-3} during the non-haze period and 6.39×10^{9} nm^2 cm^{-3} during the smoke-haze period. The mean PGMC measured was 12.43 μg m^{-3} during the non-haze period and 57.46 μg m^{-3} during the smoke-haze period. However, with the measurement of PNC by the FMPS being in the range of 5.6 to 560nm, the PSAC measurements were only made in the ultra-fine and sub-micron range. The PSAC peaks observed at 08:00, 12:00 and 17:00 during the non-hazy period, and also the peaks observed at 08:00 and 19:00 hours during the smoke-haze period can potentially be associated with the diurnal emission variations of local rush hour traffic emissions in the case of the non-haze period and a mix of local particulate emissions and transboundary aerosol particles on hazy days. These diurnal patterns were commonly reported in previous studies of the urban atmosphere (e.g. Granada, Spain) by Lyamani et al. (2008).

A statistical summary of PNC and PSAC measured during the non-haze (the pre- and post-haze periods) and the haze periods is given in Table 1 for different particle size ranges, namely the key nuclei mode from 0 to 50 nm, the ultrafine particle mode from 51 to 100 nm, and part of the submicron, accumulation particle mode from 101 to 560 nm. As can be seen from the table the mean PNC measured during the haze

period was significantly higher than that during the non-haze period in the particle size range of 51-100 nm, while the mean PSAC calculated for hazy days is smaller than that for non-hazy days in the particle size range of 0-100 nm, but almost twice higher than that in the range of 101-560 nm for non-hazy days. This observation suggests that the aerosol particles in the size range of 101-560 nm absorbed and/or scattered the incoming sunlight efficiently because of the higher surface area and thus contributed to atmospheric visibility reduction i.e. haze

Comparison of Chemical Properties of Aerosols between Non-haze and Haze Periods

Chemical characteristics of aerosols measured between non-haze and haze periods were compared and are summarized in Table 2. The proportion of the particulate-bound inorganic water-soluble ions: Cl^-, NO_3^-, nss-SO_4^{2-}, Na^+, NH_4^+ and nss-K^+ was observed to be quite similar between pre- and post-haze periods. The major contributors to the particulate mass over the non-haze period were mainly Cl^-, nss-SO_4^{2-}, and Na^+. A high proportion of Cl^- and Na^+ may potentially be derived in the form of sea salt from the open sea which is only 800 to 1000 m away from the sampling site. The presence of a high proportion of nss-SO_4^{2-} in the background air during the clear days suggests that it could be produced the atmospheric pathways involving the oxidation of SO_2 emitted from fossil fuel burning. This production pathway is conceivable since the sampling site is located in an urban area whose air quality is influenced by local traffic and industrial emissions. The non-sea salt sulfate (nss-SO_4^{2-}) was calculated as follows (Balasubramanian et al. 2003).

$$\text{nss} - SO_4^{2-} = [SO_4^{2-}] - [Na^+] \times 0.2516 \quad (1)$$

During the smoke-haze period, high mass concentrations of nss-SO_4^{2-}, NO_3^-, and NH_4^+ were observed, suggesting that these secondary inorganic aerosols were produced in the atmosphere under favourable conditions due to emissions of precursor gases from biomass burning in Indonesia (Behera et al, 2013). These places are probable locations where the peat rich grounds would provide fertile soil for future agricultural land use and motivated the recurring slash-and-burn agricultural practices in SEA. These findings are consistent with our previous observations during smoke-haze periods (Balasubramanian et al. 1999; He and Balasubramanian 2008). Indonesian peat bogs, located in Sumatra where most hotspots were identified in this

study, continue to smolder under several meters of land surface, especially during dry spells (Gras et al. 1999; Langmann and Graf 2003), releasing chemically reactive trace gases such as SO_2, NO_x and NH_3 into the atmosphere. SO_2 and NO_x are then oxidized in the atmosphere and form $(NH_4)_2SO_4$ or NH_4HSO_4 and NH_4NO_3 in the presence of NH_3 under thermodynamically favourable conditions (Behera and Balasubramanian, 2014). Moreover, the oxidation products, H_2SO_4 and HNO_3 vapors, can also bind themselves to pre-existing primary aerosols forming internally mixed smoke plumes, leading to an increase in particle size and mass concentration (See et al. 2006).

An increase in the inorganic water-soluble nss-K^+ was also observed during the smoke haze period. Being a chemical tracer for biomass (wood) and peat burning, the increase in the concentration of nss-K^+ further provide support in favour of the influences of biomass burning on the chemical composition of smoke-haze impacted aerosol particles (Currie et al. 1994). The nss-K^+ concentration was calculated from the Equation (2) below (Balasubramanian et al. 2003), and it was about 81.7 % of the total inorganic water-soluble K^+ concentration.

$$\mathrm{nss} - \mathrm{K^+} = [\mathrm{K^+}] - [\mathrm{Na^+}] \times 0.037 \quad (2)$$

Significant increments in the concentration of certain particulate-bound chemical components were observed during the smoke-haze period compared to that during the pre-haze period: NO_3^- (50 %), nss-SO_4^{2-} (74 %), Na^+ (41 %), K^+ (20%) and NH_4^+ (3 fold increase). A similar increase in their concentrations was observed based on the data obtained during the post-haze period, with the exception of K^+. The Cl^- concentration was observed to be relatively stable throughout the sampling period as it is mainly derived from the nearby marine sources. Thus, the enhancement in the concentrations of secondary inorganic aerosols $(NH_4)_2SO_4$ or NH_4HSO_4 and NH_4NO_3) appears to be associated with the long-range transboundary transport of biomass and peat burning emissions from Sumatra to Singapore. Apart from the HYSPLIT back trajectory analysis, the increase in K^+, as a biomass burning tracer, from pre-haze to smoke-haze periods can further support the above hypothesis.

Conclusions

In this study, smoke-haze episodes, caused by biomass and peat burning in Indonesia (Sumatra), were observed predominantly during the SW monsoon which lasted from 12 September 2009 to 3 October 2009. While comparing the physical characteristics of ambient aerosol particles between smoke-haze and non-haze periods, higher PSAC and PGMC were observed along with possible particle growth (aerosol aging). However, the diurnal trends in PNC showed a different pattern compared to those of PSAC and PGMC. The new particle formation phenomenon which was significant during the afternoons on non-haze days was suppressed during the smoke-haze affected period. The mean PNC trends was observed to peak at 07:00 to 09:00 and 17:00 to 19:00 due to local emissions from rush hour traffic during both smoke-haze and non-haze periods. However, a significant peak was observed in the background air in the absence of smoke haze at about 15:00 to 16:00 which could be attributed to NPF. Generally, the overall mean PNC, PSAC and PGMC measured during the smoke-haze period were higher than those during the non-hazy period. Among the 6 key particulate-bound inorganic ions investigated in this study, nss-SO_4^{2-} and NH_4^+ were observed to have the largest increase in their concentrations during the smoke haze period compared to their measurements during the non-haze period. K^+, a well-known chemical tracer of biomass and peat burning, was observed to have increased in its concentration during the smoke-haze period compared to the pre-haze period. This observation together with the back trajectory analysis suggests that the long-range transport of biomass and peat burning emissions from Indonesia to Singapore affects both the physical and chemical characteristics of aerosol particles at downwind sites. In addition, the increase in surface area of aerosols in the range of 101-560 nm together with the increase in the concentration of radiatively active secondary inorganic aerosols $(NH_4)_2SO_4$ or NH_4HSO_4 and NH_4NO_3) is indicative of the contribution of these particles to atmospheric visibility reduction during the smoke haze period. With the repeated occurrence of smoke haze episodes in SEA, there is a possibility of inducing climate change on a regional scale, which in turn could affect the hydrological cycle and thus the water budget.

Acknowledgements

The authors acknowledge the financial support from Ningbo Education Bureau, Ningbo Science and Technology Bureau, China's MOST and The University of

Nottingham. The work is also partially supported by EPSRC grant no. EP/L016362/1, Chinese National Natural Science Foundation (41303091) and Ningbo Municipal Natural Science Foundation (2014A610096).

REFERENCES

Aiken, S. R. (2004). Runaway Fires, Smoke-haze Pollution, and Unnatural Disasters in Indonesia. *Georgraphyical Review,* 94:55-79.

Balasubramanian, R., Qian, W. B., Decesari, S., Facchini, M. C., & Fuzzi, S. (2003). Comprehensive characterization of $PM_{2.5}$ aerosols in Singapore. *Journal of Geophysical Research-Atmosphere,* 108 (D16):4523, doi:10.1029/2002jd002517.

Balasubramanian, R., Victor, T., & Begum, R. (1999). Impact of biomass burning on rainwater acidity and composition in Singapore. *Journal of Geophysical Research-Atmosphere*, 104(D21): 26881-26890 , doi:10.1029/1999jd900247.

Bergin, M. H., Greenwald, R., Xu, J., Berta, Y., & Chameides, W. L. (2001). Influence of aerosol dry deposition on photosynthetically active radiation available to plants: A case study in the Yangtze delta region of China. *Geophysical Research Letters,* 28(18): 3605-3608,

Behera. S.N., Betha, R., Balasubramanian, R. (2013) Insights into chemical coupling among acidic gases, ammonia and secondary inorganic aerosols. *Aerosol and Air Quality Research*, 13: 1282 – 1296.

Behera SN and Balasubramanian, R. (2014) Influence of Biomass Burning on Temporal and Diurnal Variations of Acidic Gases, Particulate Nitrate, and Sulfate in a Tropical Urban Atmosphere. *Advances in Meteorology,* DOI: 10.1155/2014/828491.

Betha, R., Spracklen, D. V., & Balasubramanian, R. (2013). Observations of new aerosol particle formation in a tropical urban atmosphere. *Atmospheric Environment,* 71: 340-351.

Bodhaine, B. A., Ahlquist, N. C., & Schnell, R. C. (1991). Three-wavelength nephelometer suitable for aircraft measurement of background aerosol scattering coefficient. *Atmospheric Environment,* 25(10): 2267-2276.

Brook, J. R., Poirot, R. L., Dann, T. F., Lee, P. K. H., Lillyman, C. D., & Ip, T. (2007). Assessing sources of PM2.5 in cities influenced by regional transport. *Journal of Toxicology and Environmental Health-Part a-Current Issues,* 70(3-4): 191-199.

Chew, F. T., Goh, D. Y. T., Ooi, B. C., Saharom, R., Hui, J. K. S., & Lee, B. W. (1999). Association of ambient air-pollution levels with acute asthma exacerbation among children in Singapore. *Allergy, 54*(4): 320-329.

Currie, L. A., Klouda, G. A., Klinedinst, D. B., Sheffield, A. E., Jull, A. J. T., Donahue, D. J., et al. (1994). Fossil-mass and biomass combustion-C14 for source identification, chemical tracer development, and model validation. *Nuclear Instruments & Methods in Physics Research Section B-Beam Interactions with Materials and Atoms* 92(1-4): 404-409.

Davies, S. J., & Unam, L. (1999). Smoke-haze from the 1997 Indonesian forest fires: effects on pollution levels, local climate, atmospheric CO_2 concentrations, and tree photosynthesis. *Forest Ecology and Management,* 124(2-3): 137-144.

Draxler, R. R. a. R., G.D. (2013). HYSPLIT (HYbrid Single-Particle Lagrangian Integrated Trajectory) Model access via NOAA ARL READY Website (http://ready.arl.noaa.gov/HYSPLIT.php). NOAA Air Resources Laboratory, Silver Spring, MD.

Dvorska, A., Lammel, G., & Holoubek, I. (2009). Recent trends of persistent organic pollutants in air in central Europe - Air monitoring in combination with air mass trajectory statistics as a tool to study the effectivity of regional chemical policy. *Atmospheric Environment,* 43(6):1280-1287.

Erel, Y., Kalderon-Asael, B., Dayan, U., & Sandler, A. (2007). European atmospheric pollution imported by cooler air masses to the Eastern Mediterranean during the summer. *Environmental Science and Technology,* 41(15): 5198-5203.

Geresdi, I., Meszaros, E., & Molnar, A. (2006). The effect of chemical composition and size distribution of aerosol particles on droplet formation and albedo of stratocumulus clouds. *Atmospheric Environment,* 40(10): 1845-1855.

Gnanaseelan, C., & Vaid, B. H. (2010). Interannual variability in the Biannual Rossby waves in the tropical Indian Ocean and its relation to Indian Ocean Dipole and El Nino forcing. *Ocean Dynamics,* 60(1):27-40.

Gras, J. L., Jensen, J. B., Okada, K., Ikegami, M., Zaizen, Y., & Makino, Y. (1999). Some optical properties of smoke aerosol in Indonesia and tropical Australia. *Geophysical Research Letters,* 26(10): 1393-1396.

He, J., & Balasubramanian, R. (2008). Rain-aerosol coupling in the tropical atmosphere of Southeast Asia: distribution and scavenging ratios of major ionic species. *Journal of Atmospheric Chemistry,* 60(3): 205-220.

He, J., Zielinska, B., & Balasubramanian, R. (2010). Composition of semi-volatile organic compounds in the urban atmosphere of Singapore: influence of biomass burning. *Atmospheric Chemistry and Physics,* 10(23): 11401-11413.

Heil, A., & Goldammer, J. G. (2001). Smoke-haze pollution: a review of the 1997 episode in Southeast Asia. *Regional Environmental Change,* 2(1): 24-37.

Hu, Y., Odman, M. T., Chang, M. E., Jackson, W., Lee, S., Edgerton, E. S., et al. (2008). Simulation of air quality impacts from prescribed fires on an urban area. *Environmental Science & Technology,* 42(10): 3676-3682.

IPCC (2007). Climate change 2007: the physical science basis. *Agenda, 6*(07).

Jacobson, M. Z. (2004). The short-term cooling but long-term global warming due to biomass burning. *Journal of Climate,* 17(15): 2909-2926.

Jakubczyk, D., Zientara, M., Derkachov, G., Kolwas, K., & Kolwas, M. (2005). Light scattering by microdroplets of water and water suspensions. In J. Kwela, R. Drozdowski, & T. J. Wasowicz (Eds.), *5th Workshop on Atomic and Molecular Physics*. 5849: 62-69.

Kulmala, M., Vehkamäki, H., Petäjä, T., Dal Maso, M., Lauri, A., Kerminen, V.-M., et al. (2004). Formation and growth rates of ultrafine atmospheric particles: a review of observations. *Journal of Aerosol Science,* 35(2):143-176.

Langmann, B., & Graf, H. (2003). Indonesian smoke aerosols from peat fires and the contribution from volcanic sulfur emissions. *Geophysical Research Letters,* 30(11): 1547. doi:10.1029/2002gl016646.

Langmann, B., & Heil, A. (2004). Release and dispersion of vegetation and peat fire emissions in the atmosphere over Indonesia 1997/1998. *Atmospheric Chemistry and Physics,* 4: 2145-2160.

Lee, K. H., Kim, Y. J., & Kim, M. J. (2006). Characteristics of aerosol observed during two severe haze events over Korea in June and October 2004. *Atmos. Environ.* 40(27): 5146-5155.

Lyamani, H., Olmo, F., & Alados-Arboledas, L. (2008). Light scattering and absorption properties of aerosol particles in the urban environment of Granada, Spain. *Atmos. Environ.* 42(11): 2630-2642.

Lyamani, H., Olmo, F., Alcántara, A., & Alados-Arboledas, L. (2006). Atmospheric aerosols during the 2003 heat wave in southeastern Spain I: Spectral optical depth. *Atmospheric Environment,* 40(33): 6453-6464.

MSC (2001). Precursor contributions to ambient fine particulate matter in Canada : a report by the Meteorological Service of Canada.

Olson, D. A., & Norris, G. A. (2005). Sampling artifacts in measurement of elemental and organic carbon: Low-volume sampling in indoor and outdoor environments. *Atmospheric Environment,* 39(30): 5437-5445.

Page, S. E., Siegert, F., Rieley, J. O., Boehm, H. D. V., Jaya, A., & Limin, S. (2002). The amount of carbon released from peat and forest fires in Indonesia during 1997. *Nature.* 420(6911): 61-65.

Pandis, S. N., & Seinfeld, J. H. (1998). Atmospheric chemistry and physics: From air pollution to climate change. New York: Wiley.

Radzi bin Abas, M., Oros, D. R., & Simoneit, B. R. T. (2004). Biomass burning as the main source of organic aerosol particulate matter in Malaysia during haze episodes. *Chemosphere.* 55(8): 1089-1095.

Ramanathan, V., Chung, C., Kim, D., Bettge, T., Buja, L., Kiehl, J. T., et al. (2005). Atmospheric brown clouds: Impacts on South Asian climate and hydrological cycle. *Proceedings of the National Academy of Sciences of the United States of America.* 102(15): 5326-5333.

Reid, J. S., Koppmann, R., Eck, T. F., & Eleuterio, D. P. (2005). A review of biomass burning emissions part II: intensive physical properties of biomass burning particles. *Atmospheric Chemistry and Physics,* 5: 799-825.

Rolph, G. D. (2013). Real-time Environmental Applications and Display sYstem (READY) Website (http://ready.arl.noaa.gov). NOAA Air Resources Laboratory, Silver Spring, MD. .

See, S. W., Balasubramanian, R., & Wang, W. (2006). A study of the physical, chemical, and optical properties of ambient aerosol particles in Southeast Asia during hazy and nonhazy days. *Journal of Geophysical Research-Atmospheres,* 111(D10): doi:10.1029/2005jd006180.

Stohl, A. (1998). Computation, accuracy and applications of trajectories - A review and bibliography. *Atmospheric Environment,* 32(6):947-966.

Stohl, A., & Seibert, P. (1998). Accuracy of trajectories as determined from the conservation of meteorological tracers. *Quarterly Journal of the Royal Meteorological Society,* 124(549): 1465-1484.

Sundarambal, P., Balasubramanian, R., Tkalich, P., & He, J. (2010). Impact of biomass burning on ocean water quality in Southeast Asia through atmospheric deposition: field observations. *Atmospheric Chemistry and Physics,* 10(23):11323-11336.

Tang, I. N. (1996). Chemical and size effects of hygroscopic aerosols on light scattering coefficients. *Journal of Geophysical Research-Atmospheres,* 101(D14): 19245-19250, doi:10.1029/96jd03003.

Ter-Avetisyan, S., Schnurer, M., Stiel, H., & Nickles, P. V. (2003). A high-density sub-micron liquid spray for laser driven radiation sources. *Journal of Physics D-Applied Physics,* 36(19):2421-2426.

Van der Werf, G. R., Dempewolf, J., Trigg, S. N., Randerson, J. T., Kasibhatla, P. S., Gigliof, L., Murdiyarso, D., Peters, W., Morton, D. C., Collatz, G. J., Dolman, A. J., DeFries, R. S. (2008). Climate Regulation of Fire Emissions and Deforestation in Equatorial Asia. *Proceedings of the National Academy of Sciences of the United States of America,* 105(51), 20350-20355.

Wang, W. (2002). Field Investigation of Atmospheric Visibility in Singapore. A submission in partial fulfillment for the degree of Master of Engineering, National University of Singapore.

Xu, J., Bergin, M., Yu, X., Liu, G., Zhao, J., Carrico, C., et al. (2002). Measurement of aerosol chemical, physical and radiative properties in the Yangtze delta region of China. *Atmospheric Environment,* 36(2):161-173.

529 **Figure Captions**
530

531 Figure 1 Daily mean Dust Track-corrected gravimetric mass concentrations measured
532 over the entire sampling period with the identification of smoke-haze events in 2009
533
534 Figure 2 Hotspot maps in SEA and representative 96-hrs (4-days) back trajectories of
535 air masses for the sampling period from August to November in Singapore.
536 Representative Hotspots maps during (a) the pre-haze period; (b) the smoke-haze
537 period; and (c) the post-haze period; backward trajectory clusters during (d) the pre-
538 haze period; (e) the smoke-haze period; and (f) the post-haze period; (Regional
539 hotspots maps were obtained from MODIS FIRMS Web Fire Mapper)
540
541 Figure 3 Diurnal comparisons of hourly mean values for the (a) particle number
542 concentration (PNC), (b) particle surface area concentration (PSAC), and (c) particle
543 gravimetric mass concentration (PGMC) during clear (background air) and smoke-
544 haze affected days at the sampling site

545 Table 1: Statistical parameters of particle number and surface area concentrations
546 measured during non-haze and haze affected days at the sampling site
547

Diameter (nm)	0 – 50 nm		51 – 100 nm		101 – 560 nm		0 – 560 nm	
	$dN/dlogD_p$ (#/cm³)							
	Non-haze	haze	Non-haze	haze	Non-haze	Haze	Non-haze	haze
Mean	1.76E+05	1.89E+05	1.23E+05	9.81E+04	2.87E+04	5.11E+04	3.27E+05	3.38E+05
Median	1.73E+05	1.68E+05	1.29E+05	9.58E+04	2.93E+04	5.23E+04	3.26E+05	3.34E+05
SD	4.24E+04	7.86E+04	2.10E+04	2.24E+04	3.28E+03	7.71E+03	6.13E+04	9.29E+04
Min	1.29E+05	9.62E+04	9.06E+04	6.21E+04	2.30E+04	4.05E+04	2.48E+05	2.18E+05
Max	2.65E+05	3.59E+05	1.52E+05	1.37E+05	3.33E+04	6.14E+04	4.43E+05	5.37E+05
	$dS/dlogD_p$ (nm²/cm³)							
	Non-haze	haze	Non-haze	haze	Non-haze	Haze	Non-haze	haze
Mean	5.64E+08	5.08E+08	1.85E+09	1.57E+09	2.32E+09	4.30E+09	4.73E+09	6.38E+09
Median	5.60E+08	5.05E+08	1.93E+09	1.54E+09	2.37E+09	4.43E+09	4.94E+09	6.31E+09
SD	1.12E+08	1.87E+08	3.08E+08	3.22E+08	2.63E+08	8.46E+08	4.89E+08	5.99E+08
Min	4.34E+08	2.76E+08	1.35E+09	1.04E+09	1.94E+09	2.89E+09	3.74E+09	5.38E+09
Max	7.63E+08	9.14E+08	2.26E+09	2.12E+09	2.79E+09	5.42E+09	5.28E+09	7.37E+09

548 ** SD (Standard deviation) over the 24-hrs diurnal sampling period*

549 Table 2: Summary of temporal variations of mean mass concentrations of inorganic
550 water-soluble ions measured over the entire sampling period (pre-haze, smoke-haze,
551 post-haze periods)

		Anions (μg m^{-3})				Cations (μg m^{-3})			
		Cl^-	NO_3^-	SO_4^{2-}	nss- SO_4^{2-}	Na^+	NH_4^+	K^+	nss- K^+
Pre- Haze	Mean	2.97	0.54	2.85	2.42	1.72	0.15	0.48	0.42
	SD*	0.55	0.09	–	0.87	0.70	0.08	0.09	–
Smoke-Haze	Mean	2.50	0.81	4.93	4.20	2.92	0.50	0.60	0.49
	SD	0.61	0.44	–	1.56	0.75	0.41	0.32	–
Post- Haze	Mean	2.65	0.43	2.60	2.27	1.33	0.16	0.28	0.23
	SD	0.48	0.20	–	1.23	0.84	0.27	0.07	–

552 *SD: standard deviation

553

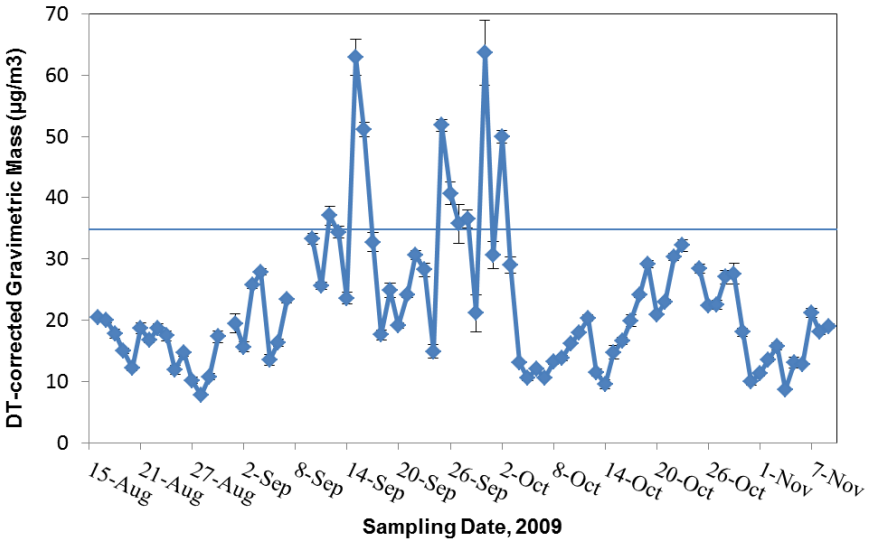

554

555 Figure 1 Daily mean Dust Track-corrected gravimetric mass concentrations measured
556 over the entire sampling period with the identification of smoke-haze events in 2009

557

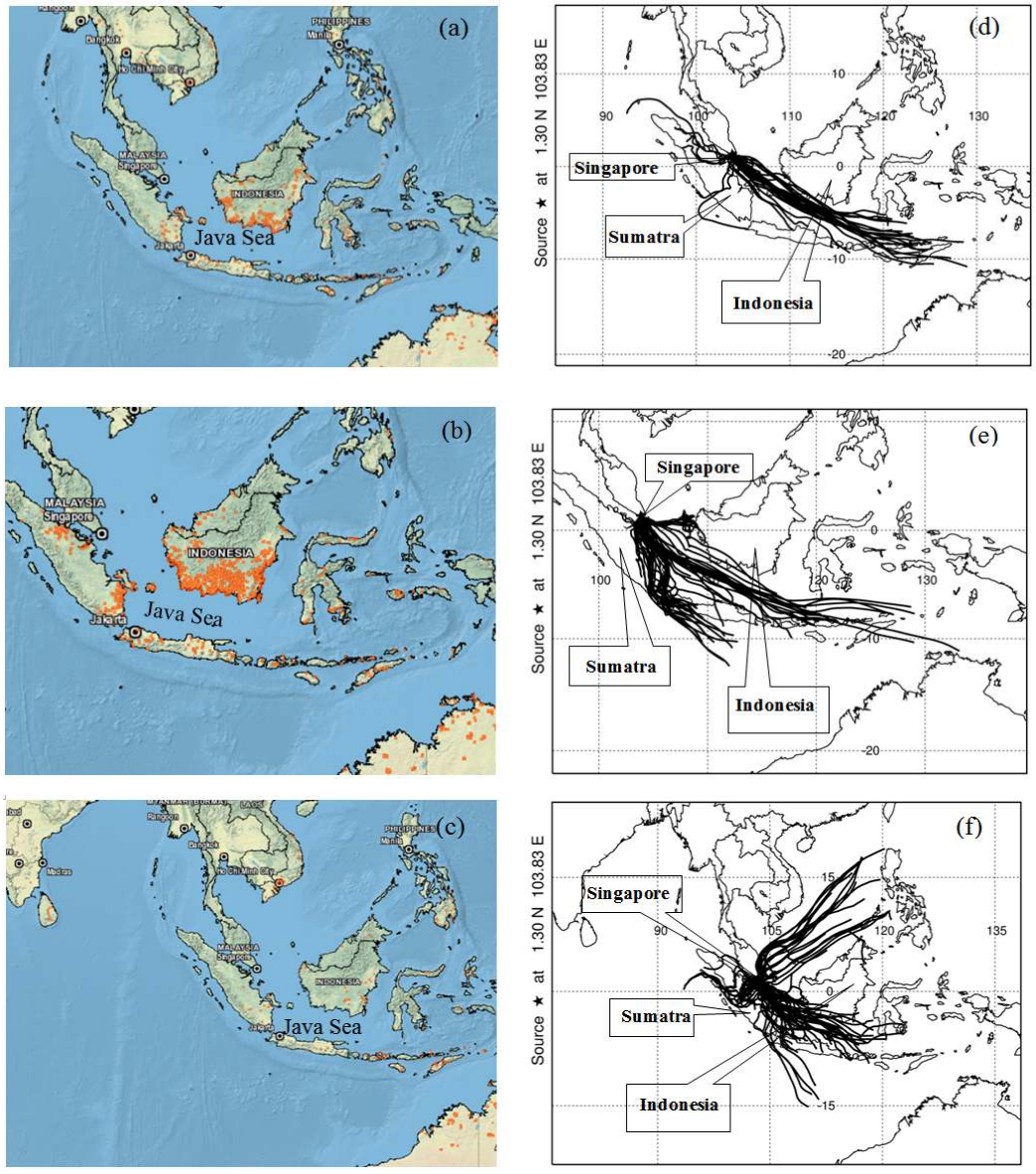

Figure 2 Hotspot maps in SEA and representative 96-hrs (4-days) back trajectories of air masses for the sampling period from August to November in Singapore. Representative Hotspots maps during (a) the pre-haze period; (b) the smoke-haze period; and (c) the post-haze period; backward trajectory clusters during (d) the pre-haze period; (e) the smoke-haze period; and (f) the post-haze period; (Regional hotspots maps were obtained from MODIS FIRMS Web Fire Mapper)

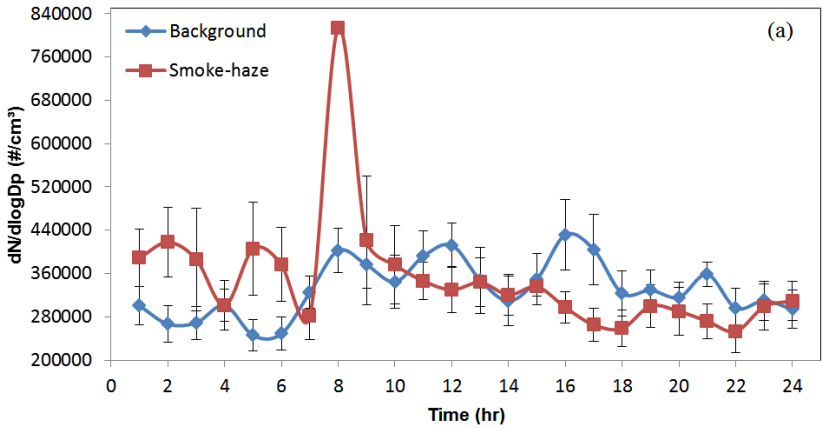

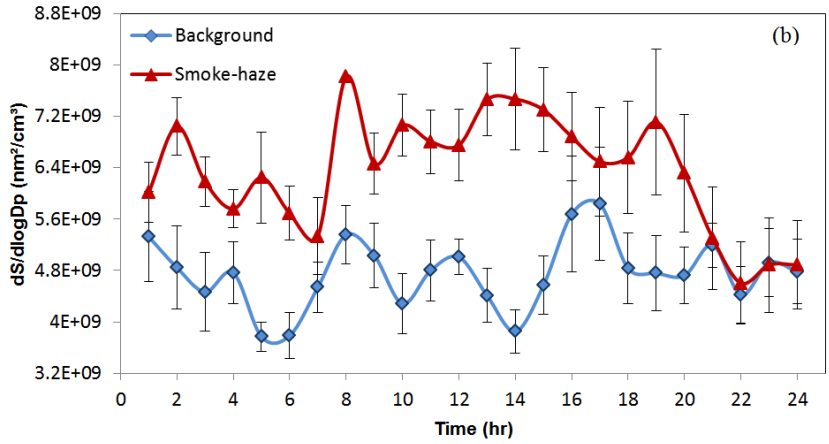

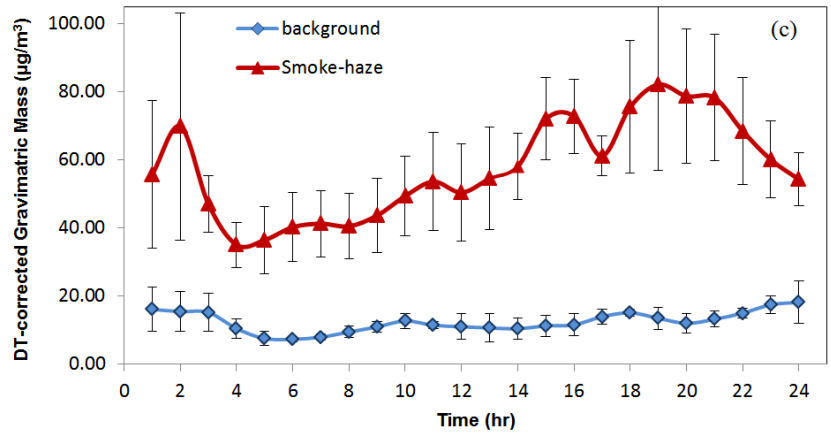

Figure 3 Diurnal comparisons of hourly mean values for the (a) particle number concentration (PNC), (b) particle surface area concentration (PSAC), and (c) particle gravimetric mass concentration (PGMC) during clear (background air) and smoke-haze affected days at the sampling site